



# Effect of microwave irradiation on the hydroxypropyl methylcellulose powder and its hydrogel studied by Magnetic Resonance Imaging

Joanna Kowalczyk\*, Jadwiga Tritt-Goc

*Institute of Molecular Physic, Polish Academy of Sciences, M. Smoluchowskiego 17, 60-179 Poznan, Poland*

## ARTICLE INFO

### Article history:

Received 16 March 2010

Received in revised form 17 July 2010

Accepted 19 July 2010

Available online 27 July 2010

### Keywords:

HPMC

MRI

Proton density

Spin–spin relaxation

Diffusion

Microwave irradiation

## ABSTRACT

Proton Magnetic Resonance Imaging (MRI) has been used to study the physical changes of hydroxypropyl methylcellulose (HPMC) hydrogels due to microwave irradiation of the polymer. The proton one-dimensional images, derived from relaxation, spin density and diffusion-weighted spin-echo experiments, provide insights on the dynamics of water and the motional state of the polymer inside the hydrogels. The obtained results indicate that the microwave irradiation causes the breaking of the HPMC polymer–hydrogen bonding network in HPMC powder which influences the dynamics of water and polymer chains within its hydrogels. In order to explain the observed spin–spin relaxation time in hydrogels composed of irradiated polymers, we have to assume that in addition to a fast exchange between the free and bound state of water also a rapid proton exchange between the water protons and the hydrogen of hydroxyl groups of side chains of the monomeric units of HPMC polymer is a major transverse relaxation mechanism.

© 2010 Elsevier Ltd. All rights reserved.

## 1. Introduction

Hydroxypropyl methylcellulose (HPMC) belongs to the industrially important class of hydro gel-forming polymers with a variety of applications. For example, HPMC is used in the pharmaceutical industry for production of coated and controlled release tablets, in the cosmetic industry as a component of body lotions, hair shampoos or ointments, serves as storage material and as structural material in plants (Gönüllü, Yener, Üner, & İncegöl, 2004; Sangalli et al., 2004). Recently, this polymer is increasingly used to produce sauces, dressings, emulsifier, and serves as a thickening agent and stabilizer in different food consumption articles (Barcenas & Rosell, 2005). The use of HPMC in the food production raises the question how micro oven heating influences the properties of the polymer itself and especially the gel produced from the irradiated polymer. This question was the inspiration of our research reported in the paper.

The HPMC, the cellulose derivative, is a linear polymer consisting of glucose repeated units linked together by  $\beta$ -1,4 glucosidic bonds with hydroxyl, methyl and hydroxypropyl groups attached to the basic unit of the polymer. The polymer chains are linked together by a network of inter- and intra-chains hydrogen bonds (Einfeldt, Meissner, & Kwasniewski, 2001). When exposed to water, the HPMC polymer forms a transparently colorless hydrogel with good stability, viscosity and texture modification.

The main goal of this paper is to present the influence of microwave irradiation on HPMC powder and the physical properties of its hydrogels. The measurements were done at room temperature for three hydrogels samples: two of them are microwave irradiated HPMC powders and the third sample non-irradiated HPMC polymer.

The method of study was Magnetic Resonance Imaging (MRI) (Blumich, 2000; Callaghan, 1991; Kimmich, 1997). MRI is very sensitive to mobile protons and can therefore study the water mobility within the gel. Furthermore, MRI is the only method which gives spatially resolved information of the nature of the process with a resolution of  $\mu\text{m}$ . The dynamics of water molecules within the hydrogels reflect the conformational changes of the HPMC polymer which are due to the microwave irradiation and the physical properties of the gel. To characterize the dynamical behavior of water we acquired in the studied hydrogels the spatially resolved spin–spin relaxations times  $T_2$  and the self-diffusion coefficients  $D$  of the water molecules along with the proton density  $\rho$ .

## 2. Experimental

### 2.1. Materials and hydrogel preparation

The studied hydroxypropyl methylcellulose polymer was purchased from FLUKA (Poznan, Poland) and used without further purification. The number-averaged molecular mass  $M_n$  is 86,000. The available data for the substitution of methoxy ( $-\text{OCH}_3$ ) and

\* Corresponding author.

E-mail address: [jak@ifmpan.poznan.pl](mailto:jak@ifmpan.poznan.pl) (J. Kowalczyk).

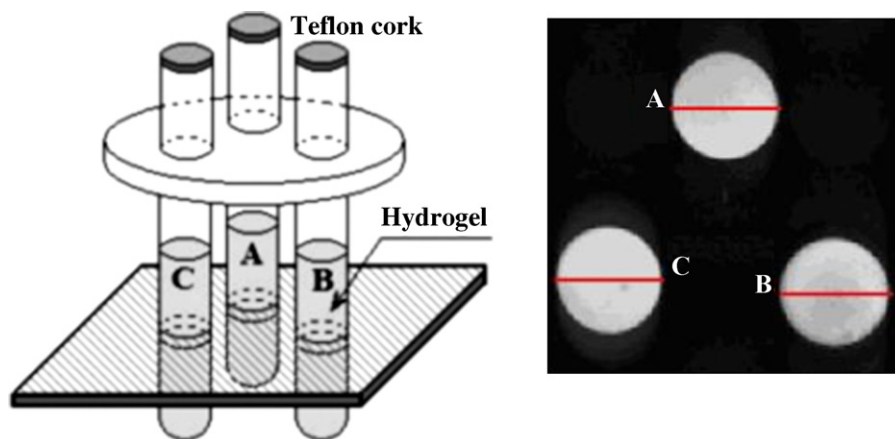


**Fig. 1.** The experimental set up diagram of the samples A, B, and C in the microimaging coil together with the corresponding images. Sample A contains 5 wt.% of hydrogels formed from non-irradiated HPMC polymer whereas the samples B and C were composed of HPMC polymer irradiated for 1 min with the microwave radiation power of 160 and 320 W, respectively. The images were acquired with a repetition time  $T_R$  of 3000 ms. The acquisition parameters were a field of view (FOV) of 30 mm  $\times$  30 mm digitized into 128  $\times$  128 pixels with a slice thickness of 2 mm (i.e. each voxel = 234  $\mu$ m  $\times$  234  $\mu$ m  $\times$  2 mm).

propylene oxide ( $-OCH_2CHCH_3$ ) groups are 29 and 7 wt.%, respectively. The average molecular weight of the repeat unit for HPMC was estimated to be about 385.

Three samples of the HPMC polymer hydrogel (samples A, B, and C) were prepared for the imaging experiments. Samples were made by addition of 0.1 g of HPMC powder to 2 g of distilled water. The gelation process started after mixing the polymer with water in the NMR glass tubes (7 mm in diameter). The samples were left at 300 K and after 23 h the transparent colorless, 5 wt.% hydrogels were obtained. The samples A, B, and C differ only in the properties of HPMC polymer. The HPMC powder used in the preparation of hydrogels B and C, prior to the gel formation, was exposed to microwave heating. Microwave irradiations were performed in a domestic microwave oven working at the frequency of 2.4 GHz. The electric power was set to 160 W for the B sample and 320 W for the C sample. The irradiation time was set to 1 min for both samples. For comparison the sample A was prepared from the non-irradiated HPMC polymer. The NMR tubes with the hydrogels were sealed to avoid the exchange between the gelatin and the atmosphere.

## 2.2. MRI measurements

MRI experiments were performed with a AVANCE 300 MHz spectrometer (Bruker, Germany) equipped with a micro imaging probehead, magnetic field gradients, and Para Vision software. A Bruker Micro 2.5 imaging probehead was used with a 25 mm bird-cage coil. This coil enables the measurement of three samples simultaneously.

Two sets of experiments were performed: the spatially resolved spin–spin relaxation times and the self-diffusion coefficient of protons in hydrogels were measured at room temperature. As a result the spin–spin-weighted and the diffusion-weighted magnetic resonance images were obtained. The images were taken for a slice from the middle of the samples, along the horizontal direction (see Fig. 1) with a repetition time  $T_R$  of 3000 ms. The acquisition parameters were a field of view (FOV) of 30 mm  $\times$  30 mm digitized into 128  $\times$  128 pixels with a slice thickness of 2 mm (i.e. each voxel = 234  $\mu$ m  $\times$  234  $\mu$ m  $\times$  2 mm).

## 2.3. Spin–spin relaxation and proton density weighted images

The spatial distribution of the spin–spin relaxation times of protons in hydrogel was studied by a single-slice multi-echo pulse sequence based on the Carr–Purcell–Meiboom–Gill (CPMG) echo

sequence ( $90^\circ - \tau - (180^\circ - 2\tau)_n$ ) with a spacing between  $180^\circ$  pulses of 9.3 ms and  $n = 128$  (Meiboom & Gill, 1958). The sinc pulse of 1 ms was used as the excitation pulse. The decay of the echo amplitude is given by the equation:

$$A(\tau) = A_0 \exp\left(-\frac{\tau}{T_2}\right) \quad (1)$$

where  $A(\tau)$  is the echo amplitude at time  $\tau$  and  $T_2$  is the spin–spin relaxation time. Eq. (1) was used to fit the experimental points of the echo amplitude decay in the acquired images pixel-by-pixel. The parameter  $A_0$  is equivalent to the spin density  $\rho(r)$  (in our case to the density of the water protons in the particular pixel of the HPMC hydrogel). Therefore, the fitting of Eq. (1) to the experimental data provides a 2D spatial distribution of the spin–spin relaxation time and proton density or so-called 2D maps of  $T_2$  and  $\rho$ . From the 2D maps the corresponding 1D profile of the studied parameters in any direction can be obtained.

The intensity of the image signal is given by the following equation (Blumich, 2000; Callaghan, 1991):

$$S = \rho(r) \left[ 1 - \exp\left\{-\frac{T_R}{T_1(r)}\right\} \right] \exp\left\{-\frac{\tau}{T_2(r)}\right\} \quad (2)$$

where  $T_1$  is the spin–lattice relaxation time and  $T_R$  the repetition time. As seen in Eq. (2) the image intensity depends on  $T_2$ ,  $T_1$  and  $\rho(r)$ . However, when the  $T_R$  is sufficiently long (five times  $T_1$ ) the  $T_1$  contrast can be eliminated from the images (Blumich, 2000; Callaghan, 1991). This condition was fulfilled in our experiments.

In Eqs. (1) and (2)  $T_2$  is called the spin–spin relaxation time. However, the quantitative true  $T_2$  values cannot be calculated in conventional microimaging experiments from a series of images with increasing echo time, because  $T_2$  is strongly affected by the self-diffusion effect (Brandl & Haase, 1994). The cumulative diffusion losses that lead to an underestimation of the  $T_2$  relaxation time can be eliminated using a modified spin-echo pulse sequence, which was theoretically justified and confirmed by the appropriate experiment.

However, in the experiments described in the paper, a conventional spin-echo pulse sequence was used. Therefore, the measured  $T_2$  values are the “apparent”  $T_{2app}$  values rather than the spin–spin relaxation time  $T_2$ . For convenience we will use the abbreviation  $T_2$  rather than  $T_{2app}$ .

### 2.3.1. Diffusion-weighted images

Diffusion-weighted images were taken using the pulse gradient spin echo (PGSE) pulse sequence introduced by Stejskal and

Tanner incorporated in the spin-warp pulse sequence (Stejskal & Tanner, 1965). It is a spin-echo pulse sequence with a pair of pulsed gradients applied before and after the refocusing  $\pi$  pulse. In the imaging version of the PGSE, a pair of pulse gradients, in the regular spin-echo imaging sequence, i.e. the diffusion weighting gradients, is included among the imaging gradients of phase encoding, slice selection, and frequency encoding. The attenuation of the echo signal due to the diffusion is described by the equation:

$$S(b_i) = S_0 \exp(-b_i D) \quad (3)$$

with the attenuation factor  $b_i$  equal:

$$b_i = \gamma^2 \delta^2 G_i^2 \left[ \Delta - \frac{\delta}{3} \right] \quad (4)$$

In Eqs. (3) and (4)  $S(b_i)$  and  $S_0$  are the echo signal intensities at  $t = 2\tau$  with and without the magnetic field gradient pulse length  $\delta$ ,  $\gamma$  is the magnetogyric ratio of the protons,  $G_i$  is the field gradient strength,  $D$  is the diffusion coefficient and  $\Delta$  is the gradient pulse interval. To obtain the  $D$  value, the  $S(b_i)$  values were measured with the changing of the field gradient strength  $G_i$ . The echo signal intensities  $S(b_i)$  were plotted against  $b_i$ . The diffusion coefficients  $D$  were calculated pixel-by-pixel by fitting Eq. (3) to these experimental points. In our experiment the field gradient strength  $G_i$  was changing from 0 to 1000 mTm<sup>-1</sup>, in equal intervals of 60 mTm<sup>-1</sup>. The gradient pulse interval  $\Delta$  and the field gradient pulse length  $\delta$  were 10 and 2 ms, respectively.

The signal intensity on the magnetic resonance images comes generally from the water protons within the gel of HPMC polymer. The polymer protons have a spin-spin relaxation time  $T_2$  too short to be observed in our imaging experiment. However, as will be shown, in some circumstances the HPMC protons can contribute to the images.

### 3. Results

#### 3.1. Effect of microwave irradiation

Fig. 1 presents the arrangement of the samples A, B, and C in the microimaging experiments together with 2D hydrogels images. The images of 2 mm slices were taken from the middle of each sample. The lines marked across the images reflected the position along which the one-dimensional profiles were acquired. Sample A contains 5 wt.% of hydrogels formed from non-irradiated HPMC polymer whereas the hydrogels in samples B and C are composed of HPMC polymer irradiated within 1 min with the microwave radiation power of 160 and 320 W, respectively. The three samples were imaged together in two series of experiments. The two-dimensional  $T_2$  and  $\rho$ -weighted tomography images of the hydrogels were obtained as the result of the first experiment. In the second experiment the  $D$  and  $\rho$ -weighted images were acquired. A representative 2D  $T_2$ -weighted images are presented in Fig. 1. From the images like that the corresponding 1D profiles of  $\rho$ ,  $D$  and  $T_2$ , of the water molecules within the studied HPMC hydrogels were obtained and are presented in Fig. 2a–c, respectively. The profiles were outlined along the diameter of samples as shown in Fig. 1. The points on the plots are an average values taken from six exactly defined volume elements (voxels) along the different diameters on 2D images. The  $T_2$ ,  $\rho$  and  $D$  parameters of gels were measured along the identical diameters of a sample, thus can be correlated quantitatively on a pixel-by-pixel basis.

Averaged profiles from Fig. 2a–c showed a quite uniform distribution of the measured parameters across the whole samples. Such homogeneous shape of the profiles indicates that the images taken were those of fully hydrated samples. The proton intensities

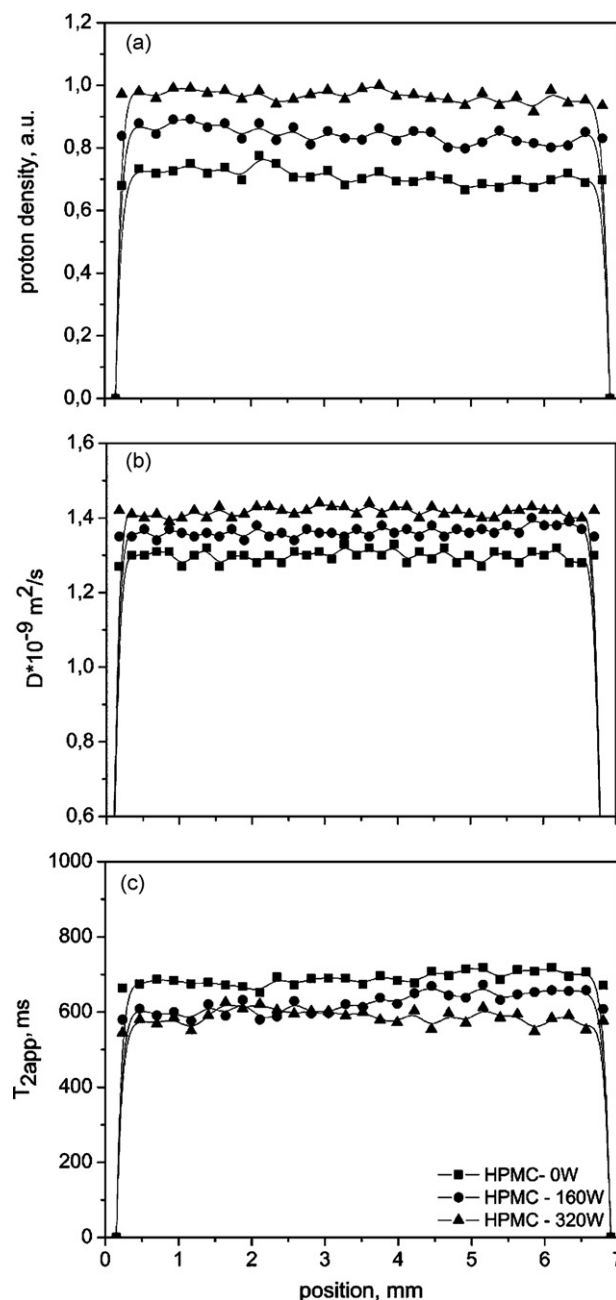


**Fig. 2.** The one-dimensional proton density profiles  $\rho$  (a), diffusion coefficient (b) and spin-spin relaxation time (c) of water within the studied HPMC hydrogels obtained for sample A (non-irradiated polymer), sample B (polymer irradiated with the microwave radiation power of 160 W) and sample C (polymer irradiated with the microwave radiation power of 320 W). The resolution of the profile is 234  $\mu$ m. The points on the plots are an average values taken from six voxels along the different diameters on 2D images from Fig. 1. The values of the standard deviation of each point are within the size of the point symbols.

and the diffusion coefficients presented in Fig. 2a and b increase with increasing the power of microwave irradiation. In the arbitrary unit the average proton intensities are equal 0.71 (sample A), 0.83 (sample B), and 0.97 for the most irradiated sample C. An average diffusion coefficient  $D$  is equal  $1.3 \times 10^{-9}$ ,  $1.36 \times 10^{-9}$ , and  $1.40 \times 10^{-9}$  m<sup>2</sup>/s, for samples A, B, and C, respectively. In contradiction, the decrease of the spin-spin relaxation is observed in the irradiating HPMC hydrogels as presented on Fig. 2c. Average  $T_2$  values are equal 680, 610 and 590 ms for A, B, and C samples, respectively.

### 3.2. Fast exchange model for water in gel

A simple two-site model can be used for the interpretation of  $T_2$  relaxation times in cellulose based materials, where water molecules are in fast diffusive exchange between interacting and non-interacting environments. The existence of the water molecules in two states as the “free” and “bound” water is widely accepted (Barbieri, Quaglia, Delfini, & Brosio, 1998; Khare & Peppas, 1993; Ono et al., 1998; Takahashi, Hatakeyama, & Hatakeyama, 2000). The bound water characterized by the spin–spin relaxation time  $T_{2b}$  is the water bound to the polymer chains by hydrogen bonds or polar interactions. The free water molecules are relatively far away from the macromolecules occupying the free volume of the polymer. However, their motions are restricted by the volume of the cavities and the spin–spin relaxation ( $T_{2f}$ ) is much faster when compared to that of the bulk. The  $T_{2b}$  is much shorter than  $T_{2f}$ .

In the studied hydrogels like in others polymer–water system the simplest relaxation mechanism involves the exchange of water protons of the pores (free water) with those of water hydrogen bounding the polysaccharide, the so-called bound water. Another possible relaxation mechanism is the chemical proton exchange between water and carbohydrate hydroxyl group of HPMC polymer. Therefore, the observed relaxation times of water within HPMC hydrogels may be accounted for by an equation as follows (Lewis & Derbyshire, 1987):

$$\frac{1}{T_{2app}} = \frac{P_b}{T_{2b}} + \frac{P_f}{T_{2f}} + \frac{P_m}{T_{2m} + k_m^{-1}} \quad (5)$$

where  $P_b$ ,  $P_f$ , are the proton fractions of bound and free water ( $P_f + P_b = 1$ ) and  $P_m$  is the fraction of macromolecular exchangeable protons with relaxation time  $T_m$ . The  $k_m$  is the first-order kinetic constant of the exchange process of the proton jump from macromolecule to the water magnetic site.

### 4. Discussion

For the studied samples mono-exponential decay of the echo amplitude was observed when measuring the relaxation and diffusion parameters. This means that water molecules within the HPMC gel are characterized by a single relaxation time  $T_2$  and diffusion constant  $D$ . Therefore, it is reasonable to assume that the water molecules of different types: free and bound are in fast diffusive exchange with respect to the chemical shift or in the intermediate exchange regime with respect to the spin–spin relaxation time (Ganapathy, Rajamohanam, Badiger, Mandhare, & Mashelkar, 2000; Quinn, McBrierty, & Wilson, 1990; Smyth, Quinn, & McBrierty, 1988; Sung, Gregonis, John, & Andrade, 1981; Yamada-Nosaka, Ishikiriya, & Todoki, 1990).

The average  $T_2$  and  $D$  values calculated for the water in studied gels are significantly lower when compared with those of pure water ( $T_2 = 2–3$  s and  $D = 2.24 \times 10^{-9}$  m<sup>2</sup>/s at 25 °C). This result is usually obtained when dealing with water relaxation and diffusion in gels or other heterogeneous systems. The reason for this is generally explained by the confinement effect. It is reasonable to assume that within the hydrogels the polymer chains together with the inter and intra-chains hydrogen bonds form a three-dimensional network encapsulating the water molecules. Thus, the water molecules in the gel are entrapped in the spaces (often called pores or voids) within the network. The confinement of the water in a gel matrix limits the molecular freedom in the gel, reduces their mobility and consequently lowers the relaxation time and diffusion coefficient.

The studied hydrogels were composed by the same amount of water and HPMC powder and differ only in the treatment of the polymer before hydration. The polymer used for the preparation of samples B and C were subject to microwave irradiation. Therefore,

the differences in the behavior of dynamic parameters and proton densities shown in Fig. 2 have to be related to the microwave irradiation. In HPMC powder the multiple hydroxyl groups on the glucose unit from one polymer chain form hydrogen bonds with oxygen molecules on the same or on a neighbor chain, holding the chains firmly together side-by-side and forming microfibrils. The microwave irradiation energy supply to the polymer powder is high enough to break the hydrogen bonds network. We anticipate that the breaking of the polymer hydrogen bonds network significantly alter the average size of the polymer voids in the hydrogel. The motion of the water reflects fundamental variations of the physical environment, inside which they diffuse. The highest value of diffusion coefficient for most irradiated polymers (see Fig. 2b) means the largest effective pore volume within hydrogels of sample C. On the other hand for the same sample also the largest proton intensity is observed as shown in Fig. 2a. This is in accordance with the assumption that for most irradiated polymers the highest breaking of the hydrogen network bond accrued. Therefore, the water which penetrates the solid HPMC during hydration inserts itself into the hydrogen-bonded links between adjacent polymer chains and such a polymer becomes most hydrated when compared to samples A and B. Consequently, the more hydrated the polymer, the more mobile the sidechains, i.e. the more plasticized are the materials. Magnetic Resonance Imaging is very sensitive to mobile protons and our images were acquired with parameters that guaranteed that the signal intensities throughout the images were directly related to the water concentration within the hydrogels. This situation takes place for sample A. However, when the mobility of the polymer increases then the polymer protons can also influence the signal intensity. This explains the observed increase in the proton signal intensity for irradiated samples B and C as shown in Fig. 2a. The behaviors of the measured values of  $\rho$  and  $D$  shown in Fig. 2a and b agree with the physical picture presented above. The viscosities of the samples also confirmed the explanation. The gel produced from irradiated polymers – samples B and C are characterized by lower viscosity than the gel of sample A. The difference in the gels viscosity was easily distinguished by a resistance test. The one-dimensional profiles of the transfer relaxation time  $T_2$  presented in Fig. 2c display different behavior than the corresponding proton density and diffusion profiles. The values of relaxation times in the hydrogels produced from irradiated HPMC polymer – samples B and C are lower than in the hydrogel composed of non-irradiated polymer – sample A. Conformational changes which are due to the microwave irradiation can alter the accessibility of the free water molecules to be bound to the polymer. As a consequence the increase of the polysaccharide chain mobility occurs which can affect a significant change in the transfer relaxation time,  $T_{2b}$ , of the protons of bound water in the gel composed from irradiated polymer and also of the hydroxyl protons of the polymer involved in water–polymer exchange. However, higher mobility indicates longer relaxation time – a situation not found in our experiment. We observe a reduction of the average values of the relaxation time in the function of microwave power. Therefore, in order to explain this fact we have to assume that in addition to a fast exchange between the free and bound state of water also a rapid proton exchange between water protons and the hydrogen of the hydroxyl groups of the side chains of the monomeric units of HPMC polymer is a major transverse relaxation mechanism in the studied hydrogels. The situation is found in other polymer systems, also for cellulose gels (Barbieri et al., 1998; Hills, Wright, & Belton, 1990; Lewis & Derbyshire, 1987; Nystrom, Moseley, Brown, & Roots, 1981; Roorda, De Bleyser, Junginger, & Leyte, 1990). In such a case the observed  $T_2$  value is expressed by Eq. (1). Unfortunately, our measurements were not able to distinguish the contributions from the particular sources of the relaxation to the measured  $T_2$  values. The chemical exchange is accelerated by the higher mobility of



the irradiated polymer chains and causes the observed lowering of the relaxation time in samples B and C. The biggest decrease of the relaxation time in sample C can be also related to the self-diffusion. This effect strongly affected the  $T_2$  value in the microimaging experiments (Brandl & Haase, 1994). We can expect the biggest influence on relaxation time in sample C because the water diffusivity in this hydrogel is the highest when compared with samples B and A.

The Electron Paramagnetic Resonance (EPR) spectra measured for the irradiated HPMC polymer were silent which means that no long live radicals were produced due to microwave irradiation.

## 5. Conclusions

We have shown that proton-imaging experiments are very useful in studying the microwave irradiation effect of HPMC polymer on the physical properties of its hydrogels. They were studied through the dynamics of water molecules as the probe molecules. The following conclusions are obtained in this study from the experimental results of water spin–spin relaxation times  $T_2$ , self-diffusion coefficients  $D$  and the proton density  $\rho$  measurements: (1) microwave irradiation causes the breaking of the HPMC polymer–hydrogen bonding network; (2) the dynamics of water and polymer chains within the HPMC hydrogels are markedly affected by the structural change of the HPMC polymer–hydrogen bonding network in solid state; and (3) in hydrogels composed of irradiated polymers, the chemical exchange process is to be considered as an important source of transverse relaxation.

## References

- Barbieri, R., Quaglia, M., Delfini, M., & Brosio, E. (1998). Investigation of water dynamic behaviour in poly(HEMA) and poly(HEMA-co-DHPMA) hydrogels by proton  $T_2$  relaxation time and self-diffusion coefficient NMR measurements. *Polymer*, 39, 1059–1066.
- Barcenas, M. E., & Rosell, C. M. (2005). Effect of HPMC addition on the microstructure, quality and aging of wheat bread. *Food Hydrocolloids*, 19, 1037–1043.
- Blumich, B. (2000). *NMR imaging of materials*. New York: Oxford Science Publications.
- Brandl, M., & Haase, A. (1994). Molecular diffusion in NMR microscopy. *Journal of Magnetic Resonance B*, 103, 162–167.
- Callaghan, P. T. (1991). *Principles of nuclear magnetic resonance microscopy*. New York: Oxford Science Publications.
- Einfeldt, J., Meissner, D., & Kwasniewski, K. (2001). Polymer dynamics of cellulose and other polysaccharides in solid state-secondary dielectric relaxation processes. *Progress in Polymer Science*, 26, 1419–1472.
- Ganapathy, S., Rajamohan, P. R., Badiger, M. V., Mandhare, A. B., & Mashelkar, R. A. (2000). Proton magnetic resonance imaging in hydrogels: Volume phase transition in poly(N-isopropylacrylamide). *Polymer*, 41, 4543–4547.
- Gönüllü, Ü., Yener, G., Üner, M., & İncegöl, T. (2004). Moisturizing potentials of ascorbyl palmitate and calcium ascorbate in various topical formulations. *International Journal of Cosmetic Science*, 26, 31–36.
- Hills, B. P., Wright, K. M., & Belton, P. S. (1990). The effects of restricted diffusion in nuclear magnetic resonance. *Magnetic Resonance Imaging*, 8, 755–765.
- Khare, A. R., & Peppas, N. A. (1993). Proton magnetic resonance imaging in hydrogels: Volume phase transition in poly(N-isopropylacrylamide). *Polymer*, 34, 4736–4739.
- Kimmich, R. (1997). *NMR tomography, diffusometry, relaxometry*. Heidelberg: Springer.
- Lewis, G. P., & Derbyshire, W. (1987). Investigation of the NMR relaxation of aqueous gels of the carrageenan family and of the effect of ionic content and character. *Carbohydrate Research*, 160, 397–401.
- Meiboom, S., & Gill, D. (1958). Modified spin-echo method for measuring nuclear relaxation times. *Review of Scientific Instruments*, 29, 688–691.
- Nystrom, B., Moseley, M. E., Brown, W., & Roots, J. (1981). Molecular motions of small molecules in cellulose gels studied by NMR. *Journal of Applied Polymer Science*, 26, 3385–3389.
- Ono, H., Hiroyuki, Y., Shigenobu, M., Kunihiko, O., Takeshi, K., & Iijima-Hideki, I. (1998).  $^1\text{H}$  NMR relaxation of water molecules in the aqueous microcrystalline cellulose suspension systems and their viscosity. *Cellulose*, 5, 231–247.
- Quinn, F. X., McBrierty, V. J., & Wilson, A. C. (1990). Water in hydrogels. 3. Poly(hydroxyethyl methacrylate) saline solution systems. *Macromolecules*, 23, 4576–4581.
- Roorda, W. E., De Bleyser, J., Junginger, H. E., & Leyte, J. C. (1990). Nuclear magnetic relaxation of water in hydrogels. *Biomaterials*, 11, 17–23.
- Sangalli, M. E., Maroni, A., Foppoli, A., Zema, L., Giordano, F., & Gazzaniga, A. (2004). Different HPMC viscosity grades as coating agents for an oral time and/or site-controlled delivery system: A study on process parameters and in vitro performances. *European Journal of Pharmaceutical Science*, 22, 469–476.
- Smyth, G., Quinn, F. X., & McBrierty, V. J. (1988). Water in Hydrogels. 1. A study of water in Poly(n-vinyl-2-pyrrolidone methyl methacrylate) copolymer. *Macromolecules*, 21, 3198–3204.
- Stejskal, E. O., & Tanner, J. E. (1965). Spin diffusion measurements: Spin echoes in the presence of a time-dependent field gradient. *Journal of Chemical Physics*, 42, 288–292.
- Sung, Y. K., Gregonis, D. E., John, M. S., & Andrade, J. D. (1981).  $^1\text{H}$  NMR studies on water in methacrylate hydrogels. *Journal of Applied Polymer Science*, 26, 3719–3728.
- Takahashi, M., Hatakeyama, H., & Hatakeyama, T. (2000). Phenomenological theory describing the behaviour of non-freezing water in structure formation process of polysaccharide aqueous solutions. *Carbohydrate Polymers*, 41, 91–95.
- Yamada-Nosaka, A., Ishikiriya, K., & Todoki, M. (1990).  $^1\text{H}$  NMR studies on water in methacrylate. *Journal of Applied Polymer Science*, 39, 2443–2452.